DIRECT OBSERVATION OF A PHONON BOTTLENECK USING BRILLOUIN LIGHT SCATTERING

W. J. Brya, S. Geschwind, and G. E. Devlin
Bell Telephone Laboratories, Incorporated, Murray Hill, New Jersey
(Received 22 November 1968)

The effective temperature of a narrow band of microwave acoustic phonons in Ni-doped MgO has been observed to rise to ~60°K while the bulk of the lattice phonons remains at the 2°K bath temperature when the Ni^{2+} spin system is saturated with resonant microwaves.

Using the technique of Brillouin scattering, we have observed directly a large nonequilibrium distribution of microwave acoustic phonons, in a relatively narrow frequency band, generated by relaxing paramagnetic ions.

In the usual description of the direct process of spin-lattice relaxation, it is assumed that the spins excited by resonant microwave radiation relax to the phonons which are in such good thermal contact with the bath (e.g., liquid helium), that the phonon excitation number $\bar{n}$ is essentially given by the thermal equilibrium value $\bar{n}_0$, corresponding to the bath temperature. However, as Van Vleck[1] pointed out many years ago, the number of lattice oscillators on speaking terms with the spins at low temperatures is limited. Consequently, if the spins relax sufficiently fast to the phonons, which in turn are unable to transport this energy rapidly enough to the bath, these phonons in a frequency band comparable with the EPR linewidth will be excited above their equilibrium value, a situation known as the phonon bottleneck. The existence of these hot phonons in a narrow band around the microwave frequency will modify the observed spin-lattice relaxation time T_1 from that to be expected under nonbottlenecked conditions. Various criteria have been used to demonstrate the existence of the bottleneck from T_1 measurements such as unusual temperature dependences,[2] e.g., $T_1 \sim 1/T^2$ rather than $1/T$ for the normal direct process; sample size and concentration dependences[3]; and nonexponential recovery of the spin system.[4] Brya and Wagner[5] recently have given even stronger evidence by observing orders-of-magnitude speedup in T_1 from an inverted spin system ascribed to a phonon avalanche. Shiren[6] also demonstrated the phonon avalanche and detected its propagation down a crystal. Even more recently, Anderson and Sabisky[7] have cited evidence for the effect by saturating a spin system at one end of a crystal and using optical circular dichroism to detect a rise in spin temperature along the length of the crystal due to bottlenecked phonons.

However, all the above-cited techniques attempt to observe these hot phonons indirectly by observing their averaged effect on a spin temperature. In contrast, the technique of Brillouin scattering[8] looks directly at the phonons and in a selective fashion by observing, from the totality of phonons, those traveling in a given direction in the crystal and lying on a particular branch of the acoustic spectrum. In addition, the intensity of the scattered light measures directly the effective temperature of these phonons.

The conventional analysis[2,4] shows that under microwave saturation of the spin system the ratio of the hot-phonon temperature $T_p{}^*$ to the equilibrium value T_B (i.e., the bath temperature) is given by

$$\sigma = \frac{T_p{}^*}{T_B} \sim \frac{n_0 \tau_{ph}}{T_1 \rho(\nu) \delta\nu}, \tag{1}$$

where n_0 is the thermal-equilibrium population difference between spin levels; τ_{ph}, the phonon lifetime; T_1, the intrinsic spin-lattice relaxation time in the absence of a bottleneck; $\rho(\nu)$, the density of phonon states; $\delta\nu$, the hot phonon bandwidth. Since $T_1 \propto v^5$ (where v is the velocity of sound) and $\rho(\nu) \propto 1/v^3$, $\sigma \propto v^{-2}$. The bottleneck, therefore, will generally be strongest for the lowest velocity acoustic mode and this fact, among other reasons, dictated the choice of phonons to be observed.

A single crystal of magnesium oxide containing 1% nickel as a substitutional impurity has been chosen for this study. The $3 \times 3 \times 6$-mm^3 sample is mounted in a cylindrical microwave cavity resonant at 25.6 GHz in the TE_{011} mode when immersed in liquid helium. A static Zeeman field is applied along a [110] crystal direction to bring the ground-state, $\Delta M_S = 1$, paramagnetic transitions of the Ni^{2+} ion ($S = 1$) into resonance with the microwaves. A reflex klystron is used to

produce cw saturation of these levels. A single-longitudinal-mode, single-frequency, argon-ion laser producing 250-mW output at 5145 Å serves as the light source for the Brillouin scattering. The laser beam enters through a hole in the bottom of the resonant cavity and traverses the sample; a high-reflectivity dielectric mirror deposited on the exit face of the sample returns the beam along its original path and out the cavity bottom. Light scattered at right angles to the laser beams is observed through a series of fine slits present in the side wall of the cavity. The scattered light is collected with an $f/7$ optical system, frequency-analyzed with a piezoelectrically scanned Fabry-Perot interferometer,[9] and detected by a cooled photomultiplier. The phototube output is then recorded using conventional pulse-counting circuitry and a multichannel analyzer for signal averaging.

The scattering geometry is illustrated in Fig. 1. The incident and reflected beams $\pm\vec{k}_i$ are directed along the longest sample dimension, while the 90° scattered radiation $\vec{k}_S$ is observed along a [111] direction; the scattering plane defined by $\vec{k}_i$ and $\vec{k}_S$ is a (110) crystal plane. Brillouin scattering from the acoustic phonons produces sidebands on the laser frequency which are determined by wave vector and energy conservation. For the incident and reflected beams, scattering arises from those phonons with wave vector $\vec{q}_A$ and $\vec{q}_B$, respectively. As the direction $\vec{q}_A$ and $\vec{q}_B$ are crystallographically inequivalent, phonons $\vec{q}_A$ and $\vec{q}_B$ from even the same acoustic branch generally occur at different frequencies. For the transverse-acoustic branch of interest to this study $\nu(q_A) = 25.6$ GHz and $\nu(q_B) = 31.3$ GHz. The phonons $\nu(q_B)$ are used to monitor the temperature of the crystal and to show that the bottleneck, which is produced by relaxing spins, is selective at 25.6 GHz, the resonant frequency of the Ni^{2+} spins in an external field of 8300 G.

Figure 1 also shows a typical scattering spectrum obtained at room temperature for the configuration described above. The Brillouin-scattered light is shifted to higher (anti-Stokes) and lower (Stokes) frequencies relative to the laser frequency corresponding to the destriction or creation of phonons, respectively. The free spectral range of the Fabry-Perot interferometer has been adjusted so that the Stokes component $\nu(q_A)$ of one interference order coincides with the anti-Stokes line $\nu(q_{A'})$ of an adjacent order. The scattering intensities observed are determined by several factors such as the elasto-optic constants, etc.; most significantly, however, the intensities of the Stokes and anti-Stokes sidebands of a given frequency are proportional to $\bar{n}+1$ and $\bar{n}$, respectively, where $\bar{n} \sim kT/h\nu$. At liquid-helium temperatures, the thermal Brillouin scattering[10] will therefore be more

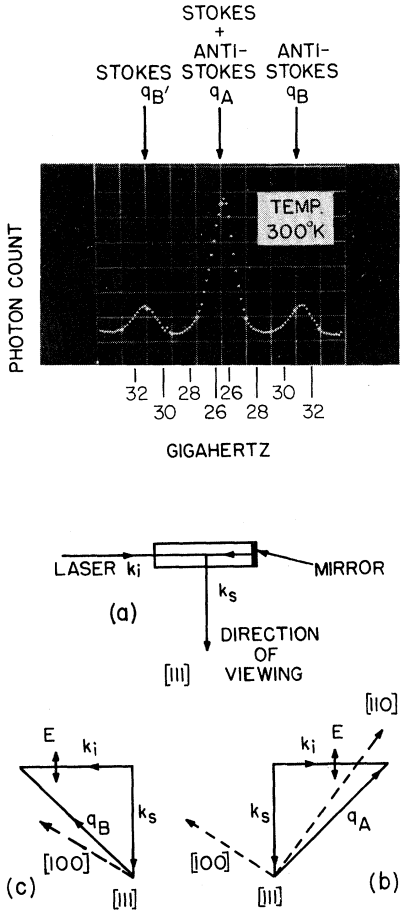

FIG. 1. 90° Brillouin scattering for MgO. (a) Incident and reflected laser beams directed along $\pm\vec{k}_i$; scattered light $\vec{k}_S$ viewed along [111] crystal direction. The scattering plane is the (110) crystal plane. (b) Scattering diagram for incident beam (laser polarization $\vec{E}$ in scattering plane); scattering arises from acoustic modes with wave vector $\pm\vec{q}_A$. Dashed lines denote principal axes of crystal. (c) Scattering diagram for reflected beam; scattering arises from acoustic modes with wave vector $\pm\vec{q}_B$. Photograph: Brillouin scattering from pure transverse-acoustic modes at wave vectors $\vec{q}_A$ and $\vec{q}_B$ in $MgO:Ni^{2+}$ at room temperature (300°K). Single sweep time is 80 msec; total integration time is 3 min. Abscissa denotes frequency shift of scattered light from laser frequency. Elastic scattering (Tyndall scattering) occurs at zero frequency shift and is not shown here. Interferometer spacing has been adjusted so that Stokes and anti-Stokes lines, from adjacent orders, for $\nu(q_A)$ overlap.

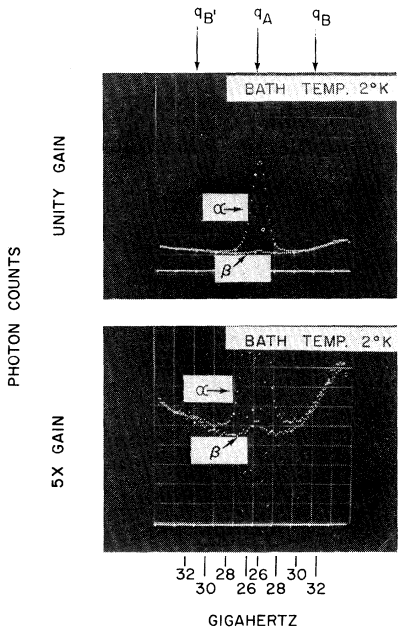

FIG. 2. Brillouin scattering in MgO:Ni^{2+} at bath temperature of 2°K. Integration time same as in Fig. 1. A magnetic field of 8300 G is applied normal to the (110) scattering plane. (α): Microwave saturation of Ni^{2+} ground state levels at 25.6 GHz. (β): No microwaves, i.e., thermal scattering at 2°K.

than two orders of magnitude weaker as shown in Fig. 2(β). Figure 2(α) shows the scattering intensity when the Ni^{2+} spin system is saturated with resonant microwaves at 25.6 GHz. It is immediately apparent that the scattering from the phonons $\nu(q_A)$ is considerably larger under microwave saturation; a comparison of the increased scattering with that of the thermal equilibrium case shows an effective temperature $\simeq 60$°K for these hot phonons. The absence of any detectable rise in the temperature of the phonons $\nu(q_B)$ above the bath temperature of 2°K, while the class $\nu(q_A)$ is heated to 60°K, indicates the selectivity of the bottleneck and suggests that it probably is occurring in a region no wider than the spin resonance linewidth of the Ni^{2+} which is approximately 500 MHz.

The heating of the phonons to 60°K is in reasonable accord with what is anticipated from Eq. (1). With a choice of values $n_0 = 3\times10^{18}$, $\tau_{ph} = 5\times10^{-7}$ sec,[11] $T_1 = 10^{-2}$ sec,[12] $\rho(\nu) = 10^4$ Hz^{-1}, and $\delta\nu = 500$ MHz, one finds $\sigma = 30$. While the values selected are reasonable, it should be borne in mind that some of these factors may be different by an order of magnitude. For example, our estimate of $\rho(\nu)\delta\nu$ is rough, as the heating of 25.6-GHz phonons on the other acoustic branches and in different crystal directions has not yet been determined.

We could not observe any splitting of the Brillouin line by spin-phonon interaction within the resolution of our apparatus which is 1.2 GHz.

Work is in progress on measuring the phonon lifetime by observing the decay rate of these hot phonons when the microwaves are switched off. We are also modifying our experimental apparatus so as to vary easily and continuously the scattering geometry which will enable us to measure the extent of heating of the other phonon branches as well as the precise hot-phonon bandwidth.

We wish to thank E. I. Gordon, J. V. Parker, and A. M. Johnson for supplying many of the laser components and advice regarding its construction; we are also grateful to A. L. Albert, W. Gronros, and L. B. Hooker for sample preparation.

---

[1]J. H. Van Vleck, Phys. Rev. 59, 724 (1941).

[2]P. L. Scott and C. D. Jeffries, Phys. Rev. 127, 32 (1962).

[3]J. A. Giordmaine, L. E. Alsop, F. R. Nash, and C. H. Townes, Phys. Rev. 109, 302 (1958); J. A. Giordmaine and F. R. Nash, Phys. Rev. 138, A1510 (1965).

[4]B. W. Faughnan and M. W. P. Strandberg, J. Phys. Chem. Solids 19, 155 (1961).

[5]W. J. Brya and P. E. Wagner, Phys. Rev. Letters 14, 431 (1965), and Phys. Rev. 157, 400 (1967).

[6]N. S. Shiren, Phys. Rev. Letters 17, 958 (1966).

[7]C. H. Anderson and E. S. Sabisky, Phys. Rev. Letters 21, 987 (1968).

[8]Excellent accounts of the Brillouin scattering technique are given by I. L. Fabelinskii, Molecular Scattering of Light (Plenum Press, Inc., New York, 1968); G. B. Benedek and K. Fritsch, Phys. Rev. 149, 647 (1966).

[9]Designed and manufactured by L. F. Mollenauer and C. D. Grandt.

[10]Sample heating due to absorption of laser light is found to be negligible at 2°K.

[11]Our choice of τ_{ph} is based on the time of flight of a phonon to the crystal boundary.

[12]The estimate of T_1 is obtained from M. F. Lewis and A. M. Stoneham, Phys. Rev. 164, 271 (1967).

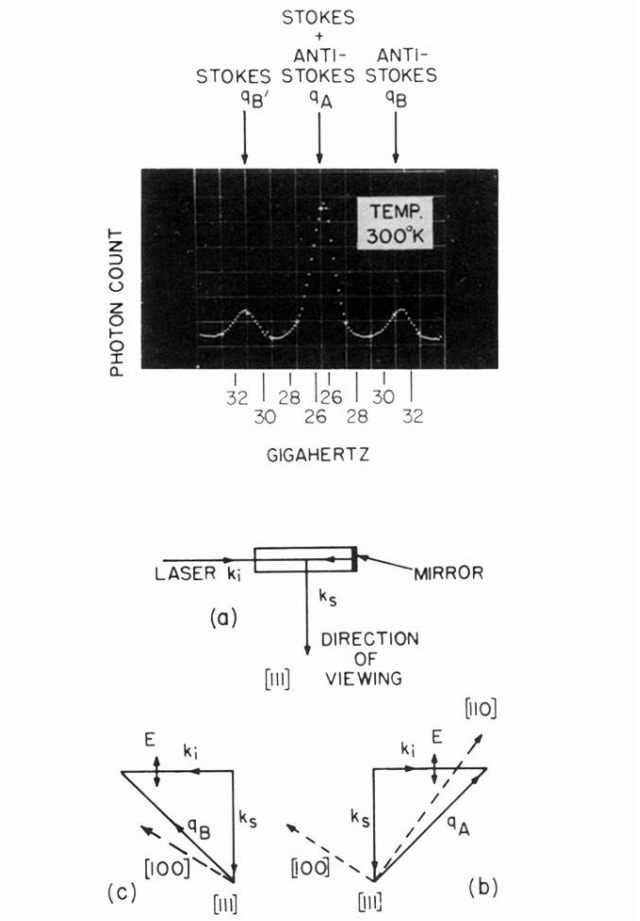

FIG. 1. 90° Brillouin scattering for MgO. (a) Incident and reflected laser beams directed along $\pm\vec{k}_i$; scattered light $\vec{k}_s$ viewed along [111] crystal direction. The scattering plane is the (110) crystal plane. (b) Scattering diagram for incident beam (laser polarization $\vec{E}$ in scattering plane); scattering arises from acoustic modes with wave vector $\pm\vec{q}_A$. Dashed lines denote principal axes of crystal. (c) Scattering diagram for reflected beam; scattering arises from acoustic modes with wave vector $\pm\vec{q}_B$. Photograph: Brillouin scattering from pure transverse-acoustic modes at wave vectors $\vec{q}_A$ and $\vec{q}_B$ in MgO:Ni^{2+} at room temperature (300°K). Single sweep time is 80 msec; total integration time is 3 min. Abscissa denotes frequency shift of scattered light from laser frequency. Elastic scattering (Tyndall scattering) occurs at zero frequency shift and is not shown here. Interferometer spacing has been adjusted so that Stokes and anti-Stokes lines, from adjacent orders, for $\nu(q_A)$ overlap.

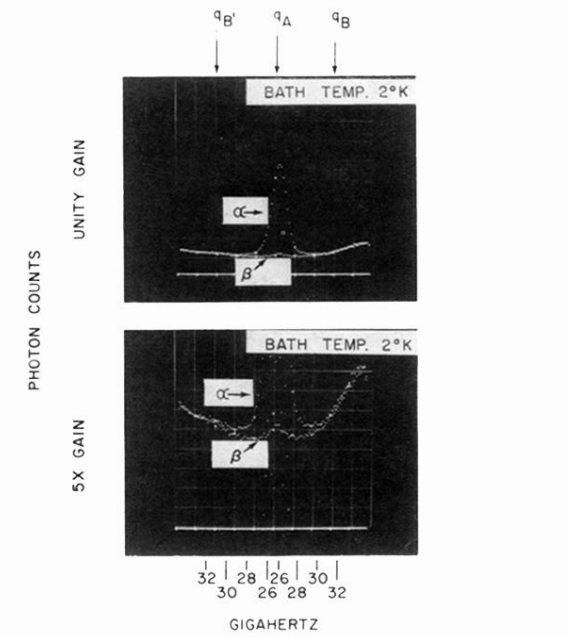

FIG. 2. Brillouin scattering in MgO:Ni^{2+} at bath temperature of 2°K. Integration time same as in Fig. 1. A magnetic field of 8300 G is applied normal to the (110) scattering plane. (α): Microwave saturation of Ni^{2+} ground state levels at 25.6 GHz. (β): No microwaves, i.e., thermal scattering at 2°K.